Thiol−Ene Free-Radical and Vinyl Ether Cationic Hybrid Photopolymerization

Huanyu Wei,† Qin Li,† Moriam Ojelade,‡ Samy Madbouly,† Joshua U. Otaigbe,† and Charles E. Hoyle*,†

School of Polymers and High Performance Materials, University of Southern Mississippi, Hattiesburg, Mississippi 39406, and Department of Natural Science, University of Houston-Downtown, Houston, Texas 77002

Received May 18, 2007; Revised Manuscript Received August 15, 2007

ABSTRACT: The photopolymerization kinetics of mixtures containing a trithiol and a trivinyl ether (in different molar ratios) with a cationic photoinitiator were investigated by real-time infrared and real-time rheology. Using this combination of real-time methods to follow both chemical conversion and rheological property development, a clear picture of physical property development during the complete polymerization process is obtained. This represents the first example of a thiol−ene radical/ene cationic two-step hybrid photopolymerization process in which thiol copolymerizes with vinyl ether functional groups in a rapid radical step growth process followed by vinyl ether cationic homopolymerization. The sequential thiol−vinyl ether copolymerization and the vinyl ether cationic polymerization result in cross-linked networks with thermal and mechanical properties that are combinations of each system.

Introduction

Studies of hybrid photopolymerization have primarily focused on overcoming the limitations of polymerization of a single type of system.[1] Hybrid polymerizations involving simultaneous or sequential polymerizations have led to the creation of a variety of novel polymers including interpenetrating polymer networks (IPNs)[2−9] and block copolymer networks.[10−12] In this context, free-radical and cationic photopolymerization has received considerate attention in recent years.[1−13] The primary motivation for such multicomponent hybrid polymerizations has been to develop a system which overcomes the limitations of each of the individual systems. For example, (meth)acrylate free-radical photopolymerizations suffer from oxygen inhibition and relatively high polymerization shrinkage, while ring-opening polymerizations (oxetanes and oxiranes) are characterized by water inhibition and low reaction rates. Decker et al.[2,3] and Jessop et al.[14] demonstrated that the oxygen sensitivity of the acrylate is reduced while its ultimate conversion is enhanced in hybrid photopolymerization of acrylates and epoxides. In addition, hybrid acrylate/epoxide systems exhibit enhancement in the resultant polymer matrix hardness compared to either neat acrylate or neat epoxide based networks. And yet the hybrid networks are more flexible than the neat epoxide polymer. Similar trends have been reported for many other hybrid monomer combinations (acrylate/vinyl ether, vinyl ether/ester).[2,4] Stansbury et al.[5] reported that the moisture sensitivity of cationic photopholymerization is also reduced in methacrylate/vinyl ether hybrid systems. Oxman et al.[15] investigated "sequential stage curable hybrid systems" involving an acrylate/cycloaliphatic epoxide combination in which the reaction system exhibits several discrete stages. Upon exposure to light, both free-radical and cationic initiating centers were produced by a three-component initiator system: the acrylate polymerized first, followed by the slower epoxide cationic polymerization. Controlling the order and timing of the sequential stages of the hybrid free-radical/cationic monomer system can be achieved either by the use of two independent initiators that are activated by distinct wavelengths of light[16,17] or the use of a single light source to create both the free-radical and cationic active centers simultaneously with chemical control over the sequential polymerization stages. This chemical control can be achieved in several ways including using two separate initiators (one a free radical, the other cationic)[3,7,9,18] or a single initiator system[10,15,19,20] that generates both free-radical and cationic initiating species. The unique set of properties afforded by hybrid photopolymerization systems make them attractive for a wide variety of applications, for example, medical systems, rapid prototyping resins,[21] advanced coatings, and adhesives.

There has been a revival of interest in thiol−ene photopolymerization in the past 5 years. It has been clearly shown that thiol−ene polymerization (including thiol and acrylate combinations) has distinct advantages over the polymerization of traditional acrylates related to the basic polymerization process including reduced oxygen inhibition, production of highly uniform cross-link density networks, and low shrinkage/induced stress during polymerization.[22] Recently, it has been shown that polymerization of acrylate and thiol−ene mixtures exhibit interesting mechanical and impact properties.[23] In the case of binary thiol−acrylate and ternary thiol−ene−acrylate systems, free-radical step growth (thiol−ene and thiol−acrylate) and free-radical chain growth (acrylate homopoloymerization) processes occur simultaneously to build up polymer networks with properties that potentially can be adapted to a wide variety of applications. In the ternary systems, since all free-radical processes occur simultaneously, chain transfer from the acrylate to the thiol−ene reaction competes with acrylate homopolymerization. In the binary thiol−acrylate systems,[24] acrylate homopolymerization reactions and thiol−acylate copolymerization reactions occur simultaneously with approximately 2−3 acrylate−acrylate addition steps occurring per thiol−acrylate reaction. The exact kinetics depends upon the exact structure and functionalilty of the acrylate. We stress that in all cases

* To whom correspondence should be addressed. E-mail: charles.hoyle@usm.edu.
† School of Polymers and High Performance Materials.
‡ Department of Natural Science.

10.1021/ma071131o CCC: $37.00
Published on Web 11/01/2007

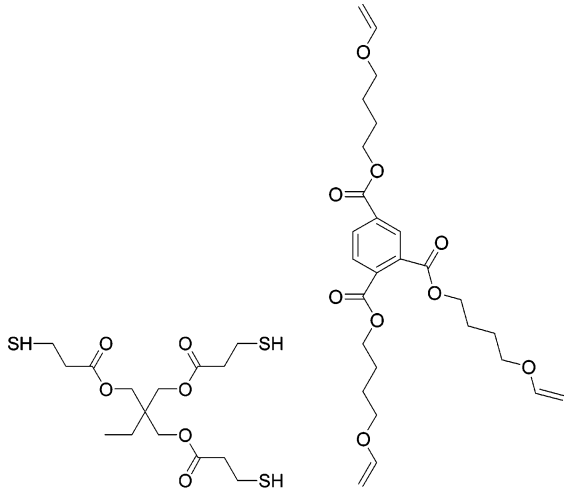

Figure 1. Chemical structures of TriThiol and TriVinyl.

involving acrylates multiple radical processes occur simultaneously.

In an effort to evaluate processes in which multiple reaction processes occur sequentially instead of simultaneously, we have turned to thiol−vinyl ether systems. In these systems, as will be shown, depending upon the concentration of each component, sequential reactions occur involving a rapid free-radical thiol−vinyl ether process followed by a cationic vinyl ether addition process. Herein, we report initial results for a thiol−vinyl ether hybrid photopolymerization system that includes a detailed kinetic, rheological, structural, and mechanical property analysis. This is the first reported example of a thiol−ene radical/cationic hybrid photopolymerization process. The results reported are indicative of the properties achievable with thiol−ene/cationic systems. The results are important since they suggest an opportunity for implementing a totally new strategy for fabricating photocurable materials for both thin film and thick cross-linked material applications. From an initially nonviscous monomer mixture, a very loose and uniform low cross-link density network with excess pendant vinyl ether groups is created by a very rapid thiol−vinyl ether free-radical polymerization followed by a subsequent cationic addition polymerization that results in a marked increase in cross-link density and formation of a unique network.

Experimental Section

Materials. Tris[4-(vinyloxy)butyl] trimellitate (TriVinyl) and trimethylolpropane tris(3-mercaptopropionate) (TriThiol) were obtained from Aldrich Chemical Co. and Bruno Bock, respectively, and used without further purification. The chemical structures of TriVinyl and the TriThiol used in this study are shown in Figure 1.The photoinitiator, CYRACURE UVI 6974, triarylsulfonium hexafluoroantimonate salts mixed with propylene carbonate, was obtained from Union Carbide Corp. TriThiol−TriVinyl mixtures were prepared by blending the trithiol into the trivinyl ether based on molar functional group concentration. The amount of UV initiator, UVI 6974, in each case, was 2 wt %. Films on glass plates (200 μm) were photocured on a Fusion curing line (10 passes) with a D bulb (belt speed of 10 ft/min, 3.1 W/cm^2 irradiance). Thick samples (1 and 4 mm) were irradiated with low-intensity 254 nm low-pressure mercury lamps (0.1 mW/cm^2 irradiance, Spectroline, model XX-15B) for 1 h in air. Samples were then cured on the Fusion curing line (10 passes for both sides).

Methods. Real-time infrared spectra (RTIR) were recorded on a modified Bruker 88 spectrometer designed to allow light penetration to a horizontal sample using a fiber-optic cable attached to a 200 W high-pressure mercury−xenon lamp source (obtained from Oriel Co.) with primary wavelengths of 313 and 366 nm and light intensity of ~1.8 mW/cm^2 (ND 2.0 filter). The real-time FTIR setup has been described in detail elsewhere.[25] Samples were prepared by mixing vinyl ether and thiol based on the moles of each functional group. Samples of 10−15 μm thickness were placed between two sodium chloride (NaCl) salt plates. UV light intensity at the sample was measured by a calibrated radiometer (International Light IL-1400). Infrared absorption spectra of samples were obtained upon continuous UV irradiation at a scanning rate of 5−10 scans/s. The vinyl ether double bonds were monitored at 1640 or 3116 cm^{-1} and the thiol group at 2575 cm^{-1}.

Real-time rheological measurements were performed using a Physica MCR 501 rheometer (Anton Paar) with a Novacure high-pressure mercury lamp with primary wavelengths of 313 and 366 nm and a light intensity of 7.5 mW/cm^2 (ND 2.0 filter). The lower fixture of the rheometer is a large quartz glass plate, while the top one is an 8 mm diameter metal plate. The sample thickness is 50 μm. The light was delivered to the sample via a liquid light pipe through neutral density filter (ND 2.0) for a given exposure time at a constant temperature (25 °C) and shear frequency (10 rad s^{-1}). Concomitant changes in viscoelastic material functions during polymerization (G', G'', and η^*) were measured as a function of exposure time. The measurements were carried out in the linear viscoelastic region (strain amplitude ≤10%).

Molecular relaxations of the films were recorded using a TA Q800 dynamic mechanical analyzer (DMA). DMA was conducted in the tensile mode for 19 × 5.6 mm size samples with thicknesses of 100−150 μm. Free-standing film samples, obtained by removing films cured by Fusion UV curing line from glass substrates, were heated from −50 to 200 °C at a rate of 3 °C/min and at a frequency of 1 Hz in air. As described in detail in a previous publication,[23] a Tinius Olsen instrument (model 92T) was modified with extensive help from the Tinius Olsen Testing Machine Co., Inc., to measure the energy absorbed upon moderate impact (1.13 Joules) with a steel head was used to investigate the impact resistances of the 4 mm thick samples. The typical sample dimensions were 80 mm × 20 mm × 8 mm ($L \times W \times H$). Two photocured 4 mm plates were pressed together back to back to eliminate any contribution from the steel plate. The striking edge of the pendulum, which complied with ASTM 12.3, was made of hardened steel, tapered to have an incline angle of 45° and rounded at the edge to a radius of 3.17 mm. Tensile property measurements were obtained with a Mechanical Testing Machine (MTS-Alliance RT/10) according to ASTM D882, using a 100 N load cell with a specimen gauge length of 40 mm at a cross-head speed of 25 mm/min. A width−thickness ratio of 8 was used for the tensile testing. Five tests were run for each sample, and an average value is reported.

Results and Discussion

This paper focuses on the hybrid photopolymerization of thiol−ene and cationic systems involving the two components in Figure 1: a trithiol (designated TriThiol) and a trivinyl ether (designated TriVinyl). Each mixture contains 2 wt % of a cationic triarylsulfonium hexafluoroantimonate photoinitiator that generates both radical and cationic species upon UV light exposure leading to the initiation of both radical and cationic photopolymerization processes.[26] A discussion of the real-time chemical kinetics and buildup of viscoelastic properties is followed by an evaluation of the final film properties of several thiol−vinyl ether combinations.

Real-Time Chemical Kinetics and Rheology. Kinetic analyses were conducted with real-time FTIR (RTIR). Resultant conversion vs irradiation time plots of the TriThiol−TriVinyl sample with 50 to 50 mol % thiol to ene functional groups (designated hereafter as 50:50 TriThiol−Trivinyl), TriVinyl, and TriThiol−TriVinyl with 25 to 75 mol % thiol to ene functional groups(designated hereafter as 25:75 TriThiol−TriVinyl) are

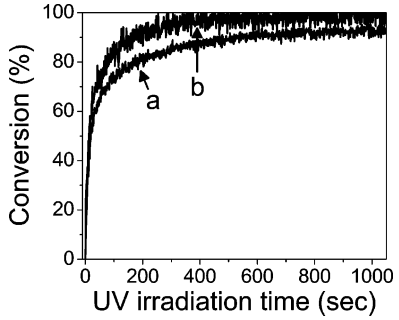

Figure 2. Real-time IR percent conversion vs time plots of 50:50 TriThiol−TriVinyl: (a) thiol and (b) vinyl ether. Irradiance (full arc) is ~1.8 mW/cm^2.

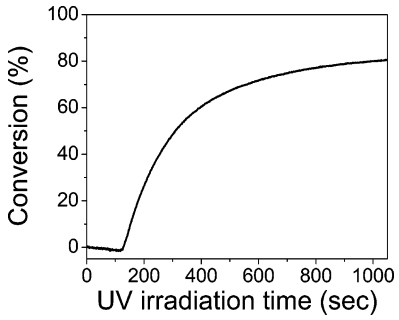

Figure 3. Real-time IR percent conversion vs time plots of pure TriVinyl. Irradiance (full arc) is ~1.8 mW/cm^2.

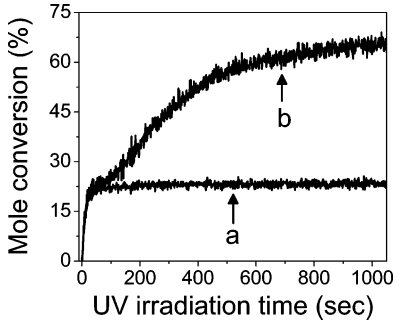

Figure 4. Real-time IR percent conversion vs time plots of 25:75 TriThiol−TriVinyl: (a) thiol and (b) vinyl ether. Irradiance (full arc) is ~1.8 mW/cm^2.

shown in Figures 2, 3, and 4, respectively. For the 50:50 TriThiol−TriVinyl system (Figure 2), the vinyl ether ene conversion was a little faster than the thiol conversion and reached almost 100% conversion (all 50 mol % of the vinyl ether ene functional groups), about 5% greater than that of the thiol conversion (95% of the original 50 mol % thiol groups reacted). This indicates that most of the polymerization proceeds by a thiol−ene step-growth radical process, with a minor contribution from the cationic polymerization of vinyl ether groups. For pure TriVinyl (Figure 3), there is about a 120 s inhibition period not seen in the 50:50 TriThiol−TriVinyl system. This is probably due in large part to the well-known moisture inhibition of cationic photopolymerization. Also, the pure TriVinyl polymerizes cationically much slower than the free-radical step growth thiol−ene polymerization of 50:50 TriThiol−TriVinyl and reaches a conversion of only about 80 mol %. When TriThiol (25 mol % thiol groups of the total moles of thiol + vinyl ether functional groups) was combined with TriVinyl (75 mol % ene groups of the total moles of thiol + ene functional groups), the thiol and vinyl ether essentially copolymerized by the thiol−ene free-radical reaction in the first 70 s (Figure 4), with about 22.5 mol % of thiol functional groups (90% of the original 25 mol % thiol groups reacted) and 23 mol % of vinyl ether ene functional groups (30.7% of the original 75 mol % ene functional groups reacted) being converted. After this initial very rapid reaction involving almost exclusively thiol−vinyl ether copolymerization, the vinyl ether continued to polymerize via a cationic polymerization process, reaching an ultimate conversion of about 67.5 mol % (90% of the original 75 mol % ene functional groups reacted). From the kinetics in Figures 4, it is apparent that a two-step hybrid photopolymerization involving an initial rapid free-radical thiol−ene polymerization and a subsequent slower cationic polymerization occurs for the 25:75 TriThiol−TriVinyl mixture with an excess of vinyl ether functional groups.

In the initial thiol−ene polymerization process, it is speculated that a very loose gel network is formed. According to the traditional gel-point equation

$$\alpha \text{ (fractional conversion at gel point)} = [1/r(f_{\text{thiol}} - 1)(f_{\text{ene}} - 1)]^{1/2} \quad (1)$$

which in the past has been applied to thiol−ene polymerization by Jacobine et al.,[27] with thiol and ene functionalities, f_{thiol} and f_{ene}, of 3 and a thiol-to-ene molar ratio based on functional groups, r, of thiol to ene of 1/3, it is predicted that the gel point should occur at ~86.6% of thiol functional group conversion. The RTIR results in Figure 4 indicate that a near- quantitative thiol conversion is attained in the initial polymerization period. This suggests that gelation occurs just at the end of the thiol−ene conversion, and thus the network formed at this point has a very low cross-link density. Then, the cationic vinyl ether homopolymerization proceeds within the framework of the initial loose gel established by the thiol−vinyl ether polymerization. To provide evidence that the thiol−vinyl ether free-radical process leads to gelation, and to provide a dynamic characterization of viscoelastic property build up during the polymerization process, we turn to real-time photorheological measurements.

Dynamic rheology is an effective method for characterizing the curing process of thermosetting polymers and for the examination of the viscoelastic properties and transition temperatures of the cured materials.[28−35] It has been applied in the past to characterization of thiol−ene photopolymerization.[36,37] The formation of polymer gels can be monitored from the time evolution of viscoelastic material functions such as G', G'', and η^*, where the entire network forming process can be divided into two parts separated by the gel point. The light exposure time dependence of the complex dynamic viscosity and storage (elastic) modulus, and η^* and G', for 50:50 TriThiol−TriVinyl, pure TriVinyl, and 25:75 TriThiol−TriVinyl at $T = 25$ °C and $\omega = 10$ rad s^{-1} are shown in Figure 5. Clearly, the results in Figure 5A,B show that the time evolution of the viscoelastic properties is strongly influenced by the concentration of TriThiol in the mixtures. Considering pure TriVinyl first, after an initial induction period consistent with the results in Figure 3, a steady rise in both η^* and G' occurs, indicating a single curing process. Although the cationic polymerization of pure TriVinyl is relatively slow, as indicated in Figure 3, a conversion of greater than 80% is achieved. Accordingly, at longer light exposure times (t > 130 s) the value of G' levels off and becomes time independent. The G' plateau value at long time is indicative of the formation of an equilibrium modulus, G_{eq}: establishment of a plateau for G' is generally accepted as the primary criterion for the formation of a stable three-dimensional polymer network.[31−33] In addition to the results for G' for TriVinyl, a

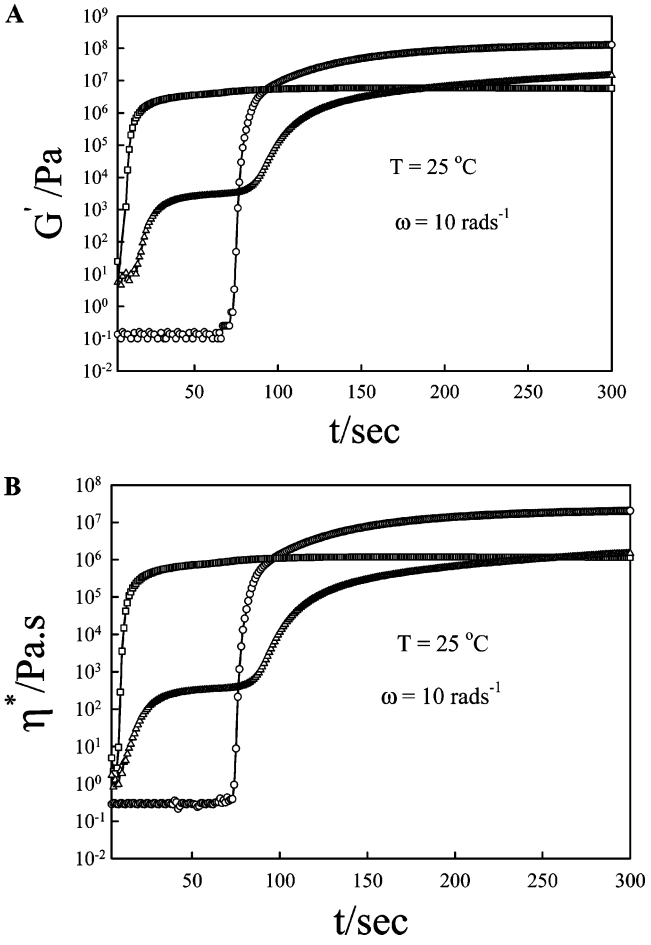

Figure 5. Time dependence of (A) dynamic storage modulus, G', and (B) complex viscosity, η^*, of different concentrations of TriThiol/TriVinyl mixtures at constant shear frequency ($\omega = 10$ rad s^{-1}) and 25 °C: ○, pure TriVinyl; △, 25:75 TriThiol−TriVinyl; □, 50:50 TriThiol−TriVinyl. Irradiance is ∼7.5 mW/cm^2.

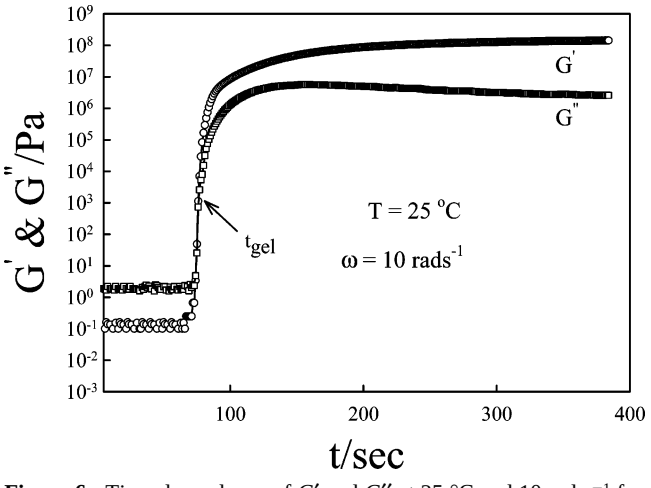

Figure 6. Time dependence of G' and G'' at 25 °C and 10 rad s^{-1} for the photopolymerization process of pure TriVinyl. The arrow shows the t_{gel} obtained from intersection point of G' and G''. Irradiance is ∼7.5 mW/cm^2.

plateau was also obtained (Figure 5B) for the complex dynamic viscosity, η^*.

As already indicated, photorheology results can be used to identify a gelation process associated with formation of network structures. We thus compare critical viscoelastic parameters for the gelation of both pure TriVinyl and 25:75 TriThiol−TriVinyl in order to provide a clear real-time rationale for rheological

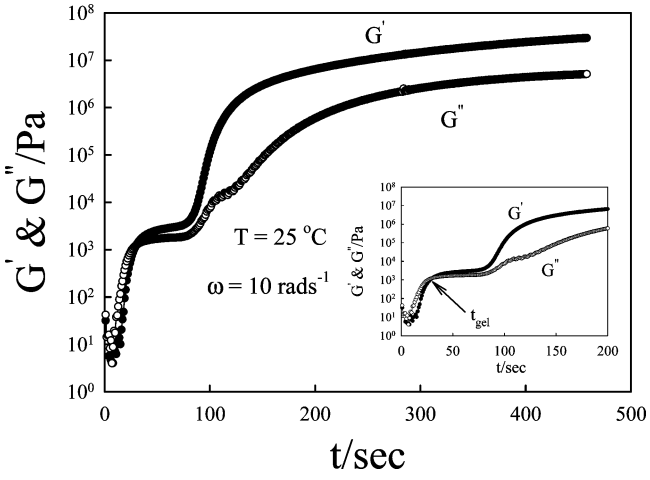

Figure 7. Time dependence of G' and G'' at 25 °C and 10 rad s^{-1} for the UV polymerization process of 25:75 TriThiol−TriVinyl. The inset plot shows the same figure at a smaller scale; the arrow shows the t_{gel} obtained from intersection point of G' and G''. Irradiance is ∼7.5 mW/cm^2.

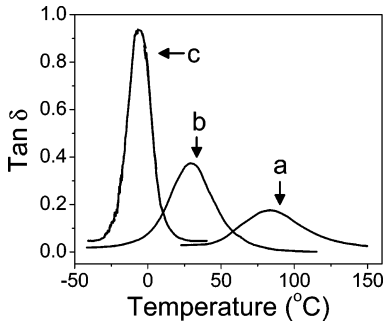

Figure 8. Plots of tan δ vs temperature for films formed from (a) pure TriVinyl, (b) 25:75 TriThiol−TriVinyl, and (c) 50:50 TriThiol−TriVinyl. DMA plots obtained with scan rate 3 °C/min and frequency 1 Hz.

property and structure development. The main goal is to provide rheological evidence for gelation at the end of an initial thiol−vinyl ether free-radical reaction for 25:75 TriThiol−TriVinyl. Figures 6 and 7 show the time dependence of G' and G'' at 25 °C and $\omega = 10$ rad s^{-1} for the TriVinyl and the 25:75 TriThiol−TriVinyl systems. First, we consider the results in Figure 6. Prior to gelation, the value of G'' for the pure TriVinyl monomer is about 1 order of magnitude greater than G'. As expected, both G' and G'' steadily increase (no intermediate plateaus) with UV light exposure, reaching approximate equilibrium values fairly rapidly after polymerization begins. The value of G', initially lower in magnitude than G'', increased more rapidly than G', becoming greater than G'' at a very short time after the polymerization begins, following the extended induction period as previously described. The early gelation process is certainly expected for multifunctional vinyl ethers. The results in Figure 7 for the 25:75 TriThiol−TriVinyl indicate that, unlike that for the pure cationic polymerization process of pure TriVinyl in Figure 6, two distinct and apparently independent processes occur. The initial process, consistent with the kinetic results for thiol−ene polymerization in Figure 4, occurs during the first 20−40 s of light exposure and leads to a pleateau in both G' and G''. More importantly, during this initial period, which as we have indicated corresponds to the free-radical thiol−vinyl ether copolymerization process, there is an intersection of the G' and G'' curves at a point that is very near to the intermediate pleateau value for each. The value for the elastic modulus G' exceeding the value for the loss modulus G''

Table 1. Mechanical Properties of TriVinyl, 25:75 TriThiol−TriVinyl, and 50:50 TriThiol−TriVinyl

	50:50 TriThiol−TriVinyl	25:75 TriThiol−TriVinyl	TriVinyl
energy absorbance (J)	0.15 (13%)	0.73 (65%)	0 (cracked)
stress at break (MPa)	1.0	3.0	3.3
strain at break (%)	13.7	13.0	1.3
energy to break (N mm/mm^3)	49.8	128.4	14.0

indicates that the sample has become an infinite gel near the end of the initial thiol−ene free-radical polymerization process as previously proposed in our discussion of eq 1. The additional increase and final plateau of G' and G'' subsequent to the initial plateau are assigned to the cationic polymerization of the vinyl ether groups that are attached to the loose thiol−vinyl ether network formed initially. In summary, the real-time photorheological measurements of the 25:75 TriThiol−TriVinyl mixture with an excess of vinyl ether functionality confirms that gelation occurs near the end of the rapid thiol−ene free-radical step-growth polymerization. The subsequent slower cationic homopolymerization of the remaining vinyl ether groups leads to additional increase in cross-link density of the network.

We note that in this paper the exact gel time has not been presented. The relatively fast polymerization kinetics of the system studied makes it impossible to evaluate the gel point from classical frequency dependencies of the viscoelastic material functions. This is supported by the time dependencies of G' and G'' (Figure 6) showing a polymerization reaction time of 15 ± 5 s. However, we made measurements of G' and G'' vs time under different shear frequencies to find out whether the crossover point is influenced by the value of shear frequency or not. These results (not shown herein) clearly indicate that the crossover point is approximately independent of the different values of shear frequency used. The behavior of the other samples was found to be similar to that of the pure TriVinyl. We thus project that the crossover point can be considered as the gel point for the specific samples of the current study.

Physical, Mechanical, and Thermal Properties of Polymerized Networks. Thermal and mechanical properties of the photopolymerized films of pure TriVinyl, 50:50 TriThiol−TriVinyl, and 25:75 TriThiol−TriVinyl mixtures were first characterized by 1 Hz DMA scans (shown in Figure 8) in the tensile mode. We first note that the DMA scan results clearly show that the 50:50 TriThiol−TriVinyl film has a very narrow tan δ peak representing a uniform network matrix resulting primarily from a free-radical thiol−ene step-growth process, while the corresponding scan for the 25:75 TriThiol−TriVinyl film is broadened and characterized by a higher temperature (just above room temperature) at the tan δ peak maximum. The results for the 50:50 TriThiol−TriVinyl network in Figure 8 are consistent with the known high uniformity of thiol−ene networks.[21,22] The film formed by polymerizing 25:75 TriThiol−TriVinyl, where both the thiol−ene free-radical and subsequent vinyl ether cationic polymerization occur, gives a sample that has a broader tan δ vs temperature plot with a peak maximum at a higher temperature than the plot obtained from the sample formed by photopolymerization of 50:50 TriThiol−TriVinyl. The broadened DMA scan for the 25:75 TriThiol−TriVinyl film is indicative of a more heterogeneous network due to the cationic chain growth process which occurs subsequent to the formation of the thiol−ene network. Results for additional TriThiol−TriVinyl ether mixtures (not shown) indicate a steady increase in the tan δ peak maximum temperature and progressive broadening with increasing vinyl ether concentration. The film produced from pure TriVinyl has a broad tan δ plot indicative of a very heterogeneous network matrix with a main peak maximum around 84 °C and a much smaller shoulder around 57 °C. It can be concluded that, from a mechanical/thermal basis, the matrix uniformity increases with TriThiol content. In order to characterize thermal transitions, DSC scans (not shown) were also recorded for the same samples. The DSC results essentially parallel the DMA results; i.e., the film from 50:50 TriThiol−TriVinyl has a very narrow glass transition region and the film from 25:75 TriThiol−TriVinyl has a broader but still distinctive transition, while the film from the strictly cationic photopolymerization of pure TriVinyl is very broad.

In view of the observation in Figures 8 that thiol−ene/cationic mixtures can be photopolymerized to give cross-linked films with relatively narrow transitions whose peak maxima can be adjusted to a given temperature by the concentration of TriThiol, an investigation of the impact resistances of 4 mm thick samples was conducted with a Tinius Olsen instrument modified to measure the energy absorbed upon moderate impact (1.13 J) with a steel head. As shown in Table 1, the photocured 25:75 TriThiol−TriVinyl sample absorbs about 65% of the impact energy of the striking head at room temperature and is more effective in dissipating impact energy than the samples of 50:50 TriThiol−TriVinyl and pure TriVinyl. The energy absorption depends on the tan δ value (at the frequency of the energy impact) at a given temperature. It is thus not surprising that the 25:75 TriThiol−TriVinyl sample has better energy-absorbing ability at room temperature where it has substantial tan δ values according to the 1 Hz DMA analysis in Figure 8. In other work,[23] it has been shown that 1 Hz DMA values provide a reasonable approximation to the impact measurements as described in the Experimental Section. Finally, it is noted that the amount of energy absorbed is greater than for traditional "energy-absorbing" materials near room temperature; i.e., commercial ethylene vinyl acetate (EVA) often used in sports applications under the same experimental conditions was found to absorb 40−50% of the 1.13 J impact energy.

The tensile mechanical properties were next evaluated for photocured 1 mm thick samples of 50:50 TriThiol−TriVinyl, pure TriVinyl, and 25:75 TriThiol−TriVinyl (Figure 9 and Table 1). Interestingly enough, the 25:75 TriThiol−TriVinyl sample, which according to the kinetic results in Figures 4, 5, and 7 involves both an initial thiol−ene free-radical and a subsequent cationic polymerization (Figure 4), has both flexibility in terms of strain at break and rigidity in terms of stress at break. This illustrates the ability of the hybrid polymerization to combine

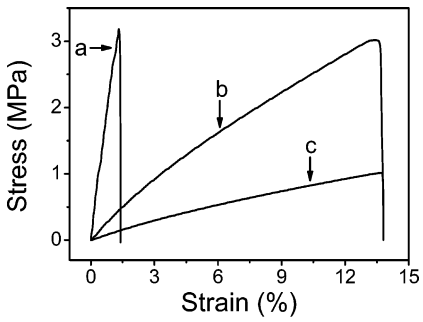

Figure 9. Tensile strain vs stress plots of 1 mm thick samples of (a) pure TriVinyl, (b) 25:75 TriThiol−TriVinyl, and (c) 50:50 TriThiol−TriVinyl.

the properties of two types of systems. The energy to break is related to the area underneath a stress−strain curve. Although energy to break is dimensionally dependent, it is one indication of material toughness. From the energy to break data in Table 1, it is clear that 25:75 TriThiol−TriVinyl has higher toughness than both 50:50 TriThiol−TriVinyl and pure TriVinyl. This is coincident with the high-energy absorption at room temperature found for the 4 mm plates made from the 25:75 TriThiol−TriVinyl.

Conclusions

In summary, real-time infrared analysis shows that the photopolymerization of a trithiol and trivinyl ether mixture with excess vinyl ether proceeds by a rapid thiol−ene radical polymerization and a subsequent cationic vinyl ether polymerization. Dynamic rheology measuremnts indicate that the 25:75 TriTthiol−TriVinyl sample gels at the end of the thiol−ene free-radical reaction followed by a cationic polymerization of residual vinyl ether groups. Mechanical property and impact measurements indicate an energy-absorbing, tough material. The results suggest an important strategy for building networks via hybrid free-radical thiol−ene/cationic−ene polymerization processes.

Acknowledgment. Financial support of this work by the MRSEC Program of the National Science Foundation under Award DMR 0213883, the Chemical and Transport System (CTS 0317646) of the National Science Foundation, and Fusion UV Systems is gratefully acknowledged. We also thank Bruno Bock for providing the thiol sample.

References and Notes

(1) Ficek, B. A.; Magwood, L.; Coretsopoulos, C.; Scranton, A. B. In *Photochemistry and UV Curing: New Trends*; Fouassier, J. P., Ed.; Research Signpost: India, 2006; Vol. 25, pp 294−300.
(2) Decker, C. *Polym. Int.* **2002**, *52*, 1141−1150.
(3) Decker, C.; Nguyen, T. V. T.; Deck, D.; Weber-Koehl, E. *Polymer* **2001**, *42*, 5531−5541.
(4) Decker, C. *Acta Polym.* **1994**, *45*, 333−347.
(5) Lin, Y.; Stansbury, J. *Polym. Adv. Technol.* **2005**, *16*, 195−199.
(6) Dean, K.; Cook, W. D. *Macromolecules* **2002**, *35*, 7942−7954.
(7) Dean, K.; Cook, W. D.; Rey, L.; Galy, J.; Sautereau, H. *Macromolecules* **2001**, *34*, 6623−6630.
(8) Dean, K.; Cook, W. D.; Zipper, M. D.; Burchill, P. *Polymer* **2001**, *42*, 1345−1359.
(9) Lin, Y.; Stansbury, J. *Polymer* **2003**, *44*, 4781−4789.
(10) Degirmenci, M.; Hepuzer, Y.; Yagci, Y. *J. Appl. Polym. Sci.* **2002**, *85*, 2389−2395.
(11) Mecerreyes, J. A.; Pomposo, J. A.; Bengoetxea, M.; Grande, H. *Macromolecules* **2000**, *33*, 5846−5849.
(12) Itoh, H.; Kameyama, A.; Nihikubo, T. *J. Polym. Sci., Part A: Polym. Chem.* **1996**, *34*, 217−225.
(13) Chen, Z. G.; Webster, D. C. *Polymer* **2006**, *47*, 3715−3726.
(14) Cai, Y.; Jessop, J. L. P. *Polymer* **2006**, *47*, 6560−6566.
(15) Oxman, J. D.; Jacobs, D. W.; Trom, M. C.; Sipani, V.; Ficek, B.; Scranton, A. B. *J. Polym. Sci., Part A: Polym. Chem.* **2005**, *43*, 1747−1756.
(16) Decker, C. *Prog. Polym. Sci.* **1996**, *21*, 593−650.
(17) Kawabata, M.; Sato, A.; Sumiyoshi, I.; Kubota, T. *Appl. Opt.* **1994**, *33*, 2152−2156.
(18) Cho, J. D.; Hong, J. W. *J. Appl. Polym. Sci.* **2004**, *93*, 1473−1483.
(19) Crivello, J. V. *J. Polym. Sci., Part A: Polym. Chem.* **1999**, *37*, 4241−4254.
(20) Crivello, J. V.; Rajaraman, S.; Mowers, W. A.; Liu, S. *Macromol. Symp.* **2000**, *157*, 109−119.
(21) Lawton, J. US Patent 6,811,937, 2004.
(22) Hoyle, C. E.; Lee, T. Y.; Roper, T. *J. Polym. Sci., Part A: Polym. Chem.* **2004**, *42*, 5301−5338.
(23) Senyurt, A. F.; Wei, H.; Phillips, B.; Cole, M.; Nazarenko, S.; Hoyle, C. E.; Piland, S. G.; Gould, T. E. *Macromolecules* **2006**, *39*, 6315−6317.
(24) Cramer, N. B.; Bowman, C. N. *J. Polym. Sci., Part A: Polym. Chem.* **2001**, *39*, 3311−3319.
(25) Lee, T. Y.; Roper, T. M.; Jonsson, E. S.; Kudyakovc, I.; Viswanathan, K.; Nason, C.; Guymon, C. A.; Hoyle, C. E. *Polymer* **2003**, *44*, 2859.
(26) Crivello, J. V.; Dietliker, K. In *Chemisty & Technology of UV & EB Formulation for Coatings, Inks & Paints*; Bradley, G., Ed.; John Wiley & Sons: New York, 1998; Vol. III, pp 326−477.
(27) Jacobine, A. F. In *Radiation Curing in Polymer Science and Technology III, Polymerization Mechanisms*; Fouassier, J. D., Rabek, J. F., Eds.; Elsevier Applied Science: London, 1993; Chapter 7.
(28) Izuka, A.; Winter, H. H.; Hashimoto, T. *Macromolecules* **1992**, *25*, 2422−2428.
(29) Adolf, D.; Martin, J. E.; Wilcoxon, J. P. *Macromolecules* **1990**, *23*, 527−531.
(30) Hodgson, D. F.; Amis, E. J. *Macromolecules* **1990**, *23*, 2512−2519.
(31) Muller, R.; Gerard, E.; Dugand, P.; Rempp, P.; Gnanou, Y. *Macromolecules* **1991**, *24*, 1321−1326.
(32) Takahashi, M.; Yokoyama, K.; Masuda, T.; Takigawa, T. *J. Chem. Phys.* **1994**, *101*, 798−804.
(33) Madbouly, S. A.; Otaigbe, J. U. *Macromolecules* **2005,** *38*, 10178−10184.
(34) Madbouly, S. A.; Otaigbe, J. U. *Macromolecules* **2006**, *39*, 4144−4151.
(35) Madbouly, S. A.; Ougizawa, T. *J. Macromol. Sci., Part B: Phys.* **2004**, *B43*, 819−832.
(36) Chiou, B. S.; English, R. J.; Khan, S. A. *Macromolecules* **1996**, *29*, 5368−5374.
(37) Chiou, B. S.; Khan, S. A. *Macromolecules* **1997**, *30*, 7322−7328.

MA071131O